DESIGN OF A HYBRID-ELECTRIC POWERTRAIN FOR A NEXT GENERATION VTOL FIREFIGHTING AIRCRAFT FROM THE DLR DESIGN CHALLENGE 2022

J. Ritter*, N. Mandry*, G. A. Can*, H. Kahlo*, B. Knoblauch*, P. Modi*, J. Schneider*, A. Strohmayer*
* University of Stuttgart, Institut for Aircraft Design, Stuttgart, Germany

Abstract

The aviation industry has always been shaped by the constant strive for improvements and state-of-the-art innovations in order to combine an economical and ecological motivation with a relentless effort to ensure safety in our skies and contribute to the well-being of our society. By using revolutionary technologies, new aircraft projects can thus contribute to fight climate change and even assist in special and demanding operations like firefighting. INtelligent FirE RespoNse Operation (INFERNO) is a fleet of four Vertical Take-Off and Landing (VTOL) aircraft operating together interconnected and intelligently for efficient, next generation aerial firefighting with an expected Entry Into Service (EIS) in 2030. The project is part of the 2022 DLR Design Challenge covering the preliminary design as well as sizing and selection of the hybrid powertrain. For the development, extensive literature research, as well as textbook methods and detailed aerodynamic simulations were utilized.

The designed aircraft is characterized by a considerable high payload ratio that features vertical take-off and landing capabilities while showing efficient horizontal flight properties with a very competitive cost basis. The 24 h operability during various weather conditions and during challenging fire scenarios is ensured using a wide variety of sensors and a modern glass-cockpit combining pilot comfort with indispensable safety aspects. Due to its modular design, every aircraft can be comfortably converted to a passenger or freight version during firefighting off-season or for cargo and crew supply during the missions.

Keywords

hybrid, electric, powertrain, aerial firefighting; aircraft design; system of systems

NOMENCLATURE

A_{prop}	Area of the vertical propellers	m^2
b	Wing span	m
C_{D}	Drag coefficient	–
C_{L}	Lift coefficient	–
D	Drag of the aircraft	N
ϵ	Glide number	–
η	efficiency	–
g	gravity constant (9.81)	m/s^2
γ	Flight path angle	deg
L	Lift of the aircraft	N
λ	Taper ratio of wing	–
m	mass of the aircraft	kg
m_{fuel}	Fuel mass	kg, lbs
μ	friction coefficient	–
P_{Cl}	Power during climb	W
P_{Cruise}	Power during cruise	W
P_{hov}	Power during hovering	W
P_{sink}	Power during descend	W
P_{TO}	Power during take off	W
P_{VTOL}	Power during vertical take off or landing	W
ρ	Density	kg/m^3
S_{W}	Wing area	m^2, ft^2
SFC	Specific fuel consumption of the aircraft	g/kWh, 1/h
$\frac{t}{c}$	Thickness ratio at wing root	–
T_{TO}	Thrust during Take off	N
v_{x}	speed of the aircraft or the air(propellers)	m s^{-1}
V_{Kr}	Fuel volume	m^3
V_{LOF}	Lift-off air speed	m/s

doi: 10.25967/570600

1. INTRODUCTION

The tremendous effects of rapidly spreading forest fires are not only characterized by destroying enormous financial assets but also by endangering people, nature, and society. Reoccurring fatalities among the civilian population and vastly destroyed neighborhoods and habitats emphasize the devastating aftermath of these natural disasters. When global warming and missing rain causes forests to dry out and thus increases the risk of wildfires, a vicious circle resulting in more and larger forest fires is inevitable [1]. While forest fires with particularly devastating dimensions have so far mainly occurred in countries like the USA or Australia, European countries are getting increasingly affected. Examples of these hazards are wildfires fires in Turkey and Greece during the summer of 2021. Even though fighting global warming as a holistic problem has to be seen as the key mission of today's generation, early and intelligent detection of wildfires and effective and quick fire response plays a crucial role while diminishing this hazard [2]. An aerial firefighting operation is especially suitable for this very purpose [3]. Nevertheless, new equipment and vehicles are needed for an increasingly effective, use case oriented fire response in regions affected today and those that will likely be affected in the coming years. The INFERNO team therefore set itself the goal of designing an Advanced Air Mobility firefighting aircraft as part of the DLR Design Challenge 2022 that has the ability to contain the forest fire significantly during the initial attack. This is achieved with a fleet of several aircraft, named after water and weather gods from various mythologies. In addition, it should be possible to take water from smaller natural sources, such as lakes and basins to increase efficiency of the mission. In order to keep production costs as low as possible and to guarantee high utilization rates, a modified version of the aircraft can operate for commercial purposes. Moreover, factors like emissions and noise reduction were considered during development to minimize the environmental footprint of the aircraft. EIS is planned for the year 2030. This paper shows the key technologies of the configuration and explains the design of the hybrid electric powertrain. Further details of the configuration and the associated design process can be found in the publication for the ICAS Congress 2022. [4].

2. DESIGN PROCESS

In the following chapter, the design process for the INFERNO aircraft is described. Therefore, crucial design decisions concerning the flight capabilities, the energy storage and the overall configuration are presented and justified. Due to the Maximum Take-Off Mass (MTOM) of less than 5670 kg and a single pilot operation, a certification under EASA CS-23 and FAR Part 23 is seeked.

2.1. Vertical Take-Off and Landing vs. Short Take-Off and Landing

In the first step of the design process, the advantages of a VTOL as well as a Short Take-Off and Landing (STOL) were evaluated. The VTOL has the major advantage that no runway is needed for take-off. This means that smaller water surfaces can be used for water refilling. The possibility of using small water sources is a clear advantage in fighting forest fires, because the time between water drops can be reduced [4]. In addition, hovering is possible and lower flight altitudes can be achieved. In favor of a configuration with STOL characteristics is the fact that the cruising speed is significantly higher and the payload share in relation to the Maximum Take-Off Weight (MTOW) is increased. In addition, the power requirement for the same payload is lower than for a VTOL vehicle [5]. This also means that operation and production is cheaper. To decide between these two concepts, the INFERNO team set the design requirement of combining the advantages of both concepts. This is achieved with the help of an electric drive concept, which offers significantly more degrees of freedom in the design of configurations. Due to the small space requirements of electric motors, they can be positioned flexibly or a larger number of small propellers can be used [6]. This leads to improved drive efficiency. Flexible positioning means that swivelling thrusters for vertical take-off and landing can be dispensed, resulting in a significant reduction in maintenance. In addition, a buffer storage allows the power required for short periods to be significantly higher than the available continuous power of the engine.

2.2. Fuel Type and Energy Storage Concept

The source of the electrical energy is subsequently examined in more detail. In order to be able to provide the necessary electrical power, various energy storage concepts are available. In the following, four promising methods for energy supply are evaluated:

- Turbogenerator operated with synthetic fuel / kerosene (an internal combustion engine generates shaft power, which is converted to electrical power + buffer battery)
- Turbogenerator operated with hydrogen (an internal combustion engine generates shaft power, which is converted to electrical power + buffer battery)
- Battery (the sole energy storage and power source are batteries)
- Fuel cell (the electric power is produced by a chemical reaction of hydrogen and oxygen + buffer battery)

The comparison is based on six categories (cf. tab. 1). Unlike the turbogenerators and fuel cell, the battery does not have to convert the energy to electricity first,

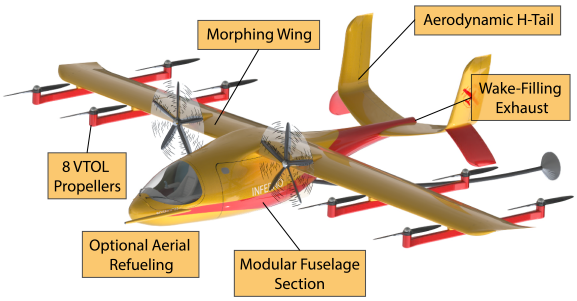

FIG 1. Unique characteristics of INFERNO

therefore it is the most efficient solution. Due to the low gravimetric energy density of current lithium-ion cells compared to kerosene and synthetic fuels and the higher weight of hydrogen tanks compared to conventional integral tanks, the turbogenerator with synthetic fuel or kerosene has the biggest weight advantage. INFERNO is designed to be used on very small rural airstrips that have limited infrastructure and might not have high voltage powerlines or hydrogen infrastructure by 2030. The main goal of the design is it to make INFERNO as versatile and agile as possible. By using synthetic fuel or kerosene and vertical take-off and landing, a base could theoretically be a large plain field with a tank truck for refueling. Thus, the turbogenerator with synthetic fuel or kerosene therefore has a big advantage over batteries and hydrogen. Furthermore it is very well known, has a high technology readiness level (cf. tab. 3) and an established supply chain in the aerospace market, which decreases costs and risk during development and EIS. The environmental impact however is due to its consumption of fossil fuels (if fueled with kerosene) or the high energy consumption during the production of synthetic fuel higher than for batteries (that can be recycled [7]) or a hydrogen burning turbogenerator. Because fuel cells do not use combustion, their environmental impact is the lowest. Overall, the dual-fuel turbogenerator powered by synthetic fuel is the most suitable technology for the INFERNO concept and its requirements. It offers the best balance between efficiency, weight, cost and availability. Especially the flexibility in operation with fast refueling, easy availability and transportability of the fuel is a key argument for the use of a carbon-based fuel.

2.3. Configuration Selection and Key Technologies

To combine VTOL and STOL capabilities, a wing like that of a classic fixed-wing aircraft is indispensable. For the positioning of the wing, a high wing is almost without alternative for amphibian aircraft, as it provides more ground clearance and distance to the water during scooping [8]. There were several options for the distribution of the drives, as the electric drives offer substantive flexibility. One option was the usage of tilt rotors but the concept requires more maintenance and is more susceptible to faults and therefore results in more costs. Moreover, the EIS of 2030 has to be considered during the design decisions. Thus, the INFERNO aircraft features separated propulsion systems for both vertical and horizontal flight. As shown in fig. 1, the final configuration selection is characterized by eight VTOL propellers distributed along the wing span to achieve sufficient rotor area. For the positioning of the propulsion, three options were investigated. The first option was the positioning at the rear of the tail as a pusher. Moreover, the positioning at the wingtips or classically close to the fuselage was evaluated. The pusher configuration caused ground clearance problems during take-off when the aircraft is rotating conventionally, so it was not suitable for the requirements. When comparing the other configurations, there were advantages for both. However, the advantages of the close-to-fuselage drive, and the associated support of the tail by the propeller wake, outweighed those of the wingtip propellers. When selecting the tail unit, the decision was made in favor of an H-tail unit. Since the rudder area became very large due to the short lever arm and the relatively high wing area, an H-tail has decisive benefits as it divided this area into two separated rudders, thus reducing the height. A more detailed investigation takes place in [4]. Fig. 1 and fig. 2 show the key characteristics, equipment and technologies of the INFERNO concept. Moreover, the aircraft dimensions are summarized in tab. 2 and fig. 4, 5 and 3.

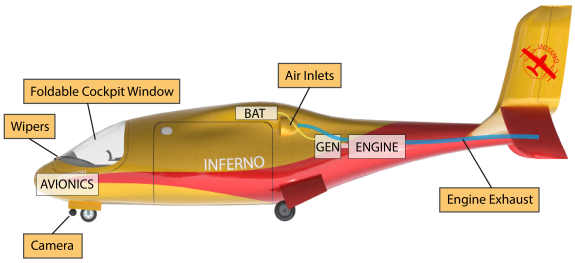

FIG 2. Unique characteristics of INFERNO 2

Tab. 3 summarizes the key technologies of INFERNO. Additionally, sources are listed for the respective Technology Readiness-Levels (TRLs) that show the technical status and further development up to 2030.

2.4. Propulsion and Battery

The VTOL and conventional option for take-off and landing leads to increased demands on the powerplant and engines. In the following chapter, the power demand is discussed and the selected hybrid configuration and energy management system is presented.

2.4.1. Calculation of Power Demand

This calculation of the power demand in the various flight phases form the basis for the subsequent sizing of the powertrain. All calculations were done according to "Flugzeugentwurf I" by Prof. Strohmayer [18], "General aviation aircraft design: Applied methods

TAB 1. Trade-off study of energy provision concepts; best: ++, worst - -

	Turbogenerator (synthetic fuel)	Turbogenerator (hydrogen)	Battery	Fuel Cell
Efficiency	0	0	++	+
Weight	+	0	–	-
Infrastructure	++	-	0	-
Costs	+	0	-	–
Environmental impact	-	+	+	++
Technology readiness	+	0	0	-
Result	+4	0	0	-1

TAB 2. Technical data of INFERNO

Aircraft Data	
Length	8.50 m
Height	3.60 m
MTOM	5670 kg
Wing Area	27.4 m^2
Aspect Ratio	9.34
Anhedral	-2°
Sweep Leading Edge	5°
Taper Ratio	0.5
Take-off Field Length	600 m
Climb Rate (hor.)	1400 ft/min
Climb Rate (VTOL)	1000 ft/min
Climb Gradient All Engines Operative (AEO)	max. 20%
Climb Gradient One Engine Inoperative (OEI)	6%
Cruise Speed	Ma 0.25
Cruise Altitude	FL 080
Glide Ratio	16.32
Fuel Consumption Design Mission	400 kg

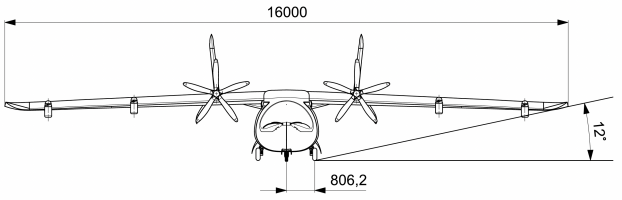

FIG 3. Front view of INFERNO

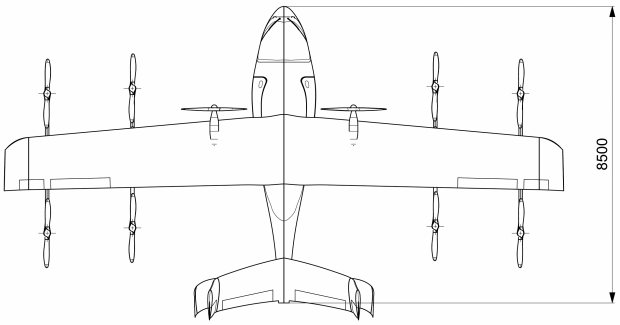

FIG 4. Top view of INFERNO

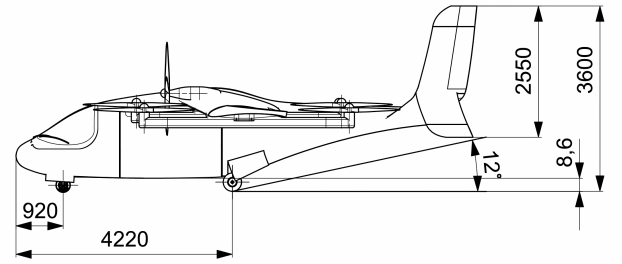

FIG 5. Side view of INFERNO

TAB 3. TRL of key technologies

Key Technology	TRL
Synthetic fuels	6 [9]
Battery	5 [10]
Wake-Filling	3-4 [11]
Hybrid system	6 [12]
Morphing Wing	6 [13]
Exchangeable fuselage	4 [14]
Electric Motors	4 [15]
Sensing Instruments	6 [16][17]

and procedures" by Gudmudsson [19] and "Grundlagen der Hubschrauber Aerodynamik" by van der Wall [20] for vertical flight. The formulas that were used during the various flight phases are shown below. For all propellers a propeller efficiency of 85% ([19]) and an electric motor efficiency of 95% ([21], [22]) was estimated.
In operation, the vertical propellers can be used during take-off as well. With intelligent thrust vectoring, the required down force at the horizontal tail can be reduced. The effects of this on the wing aerodynamics however need further testing and detailed Computational Fluid-Dynamics (CFD)-Simulations. In Fig. 6 the power demand is displayed for horizontal and vertical flight. The power demand decreases over time, because the aircraft gets lighter after it burns the fuel. This could also be used to increase the amount of water that is being scooped from the water body. Measuring this however is very difficult and should only be done, when enough operational experience with the aircraft is gathered. Furthermore it can be seen, that the vertical take-off and landing consumes way more power than the horizontal flight. Therefore the maximum amount of water, that can be carried during these flight phases is limited to 2000 kg.
Depending on the distance between the base and the fire, and the fire and the water body, it can be more efficient to start at the base with empty water tanks. In the design mission, this could safe up to 24 kg of fuel. But because at wild fires, the time until the first attack is crucial, the aircraft was filled with water at the base.

Horizontal Take-off Run:

Calculation of Lift-off speed:

$$V_{\mathrm{LOF}} = 1.1 \cdot \sqrt{\frac{2 \cdot m \cdot g}{\rho \cdot S_{\mathrm{W}} \cdot C_{\mathrm{Lmax}}}} \tag{1}$$

Calculation of acceleration during take-off run:

$$\frac{\mathrm{d}V}{\mathrm{d}t} = \frac{{V_{\mathrm{LOF}}}^2}{2 \cdot l_{\mathrm{to}}} \tag{2}$$

Lift at average airspeed:

$$L = \frac{\rho}{2} \cdot v^2 \cdot S_{\mathrm{W}} \cdot C_{\mathrm{L}} \tag{3}$$

Drag at average airspeed:

$$D = \frac{\rho}{2} \cdot v^2 \cdot S_{\mathrm{W}} \cdot C_{\mathrm{D}} \tag{4}$$

Thrust during take-off run:

$$T_{\mathrm{TO}} = \frac{\mathrm{d}V}{\mathrm{d}t} \cdot m + D + \mu \cdot (m \cdot g - L) \tag{5}$$

Calculation of power during take-off run:

$$P_{\mathrm{TO}} = T_{\mathrm{TO}} \cdot \frac{V_{\mathrm{LOF}}}{\sqrt{2}} / \eta_{\mathrm{prop,EM}} \tag{6}$$

Horizontal Climb:

Calculation of power during climb in horizontal flight:

$$P_{\mathrm{Cl}} = (\sin\gamma + \epsilon) \cdot v_{\mathrm{climb}} \cdot m \cdot g / \eta_{\mathrm{prop,EM}} \tag{7}$$

Cruise:

Calculation of power during cruise flight:

$$P_{\mathrm{Cruise}} = (\epsilon \cdot \frac{m \cdot g}{v_{\mathrm{cruise}}}) / \eta_{\mathrm{prop,EM}} \tag{8}$$

Calculation of fuel consumption during cruise flight (brequet equation):

$$m_{\mathrm{fuel}} = m - \frac{m}{\exp(l \cdot SFC \cdot \epsilon / \eta_{\mathrm{prop,EM}})} \tag{9}$$

Horizontal Descend :

Calculation of power during descend in horizontal flight mode:

$$P_{\mathrm{sink}} = \epsilon - \sin\gamma \cdot m \cdot g \cdot v_{\mathrm{sink}} \tag{10}$$

Hovering:

Calculation of required power for hovering:

$$P_{\mathrm{hov}} = m \cdot g \cdot \sqrt{\frac{m \cdot g}{2 \cdot \rho \cdot A_{\mathrm{prop}}}} / \eta_{\mathrm{prop,EM}} \tag{11}$$

Vertical Ascend and Descend:

Calculation of required power for vertical flight

$$P_{\mathrm{VTOL}} = \frac{P_{\mathrm{hov}}}{\frac{v_{\mathrm{i}}}{v_{\mathrm{i0}}}} / \eta_{\mathrm{prop,EM}} \tag{12}$$

$$\frac{v_{\mathrm{i}}}{v_{\mathrm{i0}} = -\frac{v_{\mathrm{vert}}}{2 \cdot v_{\mathrm{i0}}} + \sqrt{(\frac{v_{\mathrm{vert}}}{2 \cdot v_{\mathrm{i0}}})^2 + 1}} \tag{13}$$

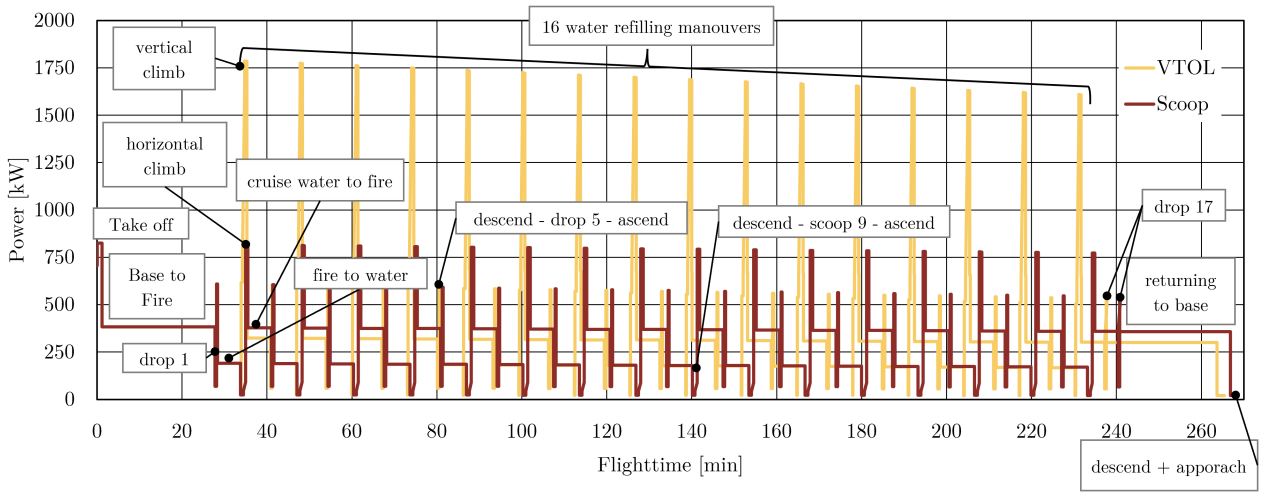

FIG 6. Power demand for the horizontal and vertical propellers during horizontal and vertical flight

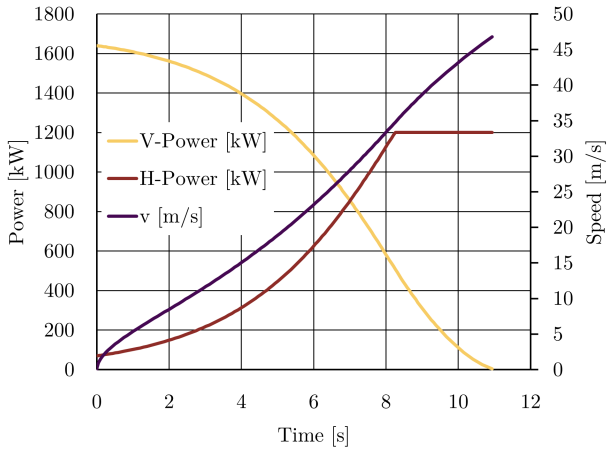

FIG 7. Power demand during transition between vertical and horizontal flight

$$v_\mathrm{i} = \sqrt{\frac{m \cdot g}{2 \cdot \rho \cdot A_\mathrm{prop}}} \tag{14}$$

For vertical descending the same formula is used with a negative vertical speed.

2.4.2. Transition between Vertical and Horizontal Flight

One of the most critical flight phase is the transition between vertical and horizontal flight. In order to safe fuel, the transition should be done as low as safely possible. In this phase, the morphing wing has its high-lift profile and hovers with its vertical propellers. Fig. 7 shows the power demand during the transition between vertical and horizontal flight.
The limiting factor is the maximum of 1800 kW electrical power that the powertrain can provide (1200 kW from the battery and 600 kW form the engine). The horizontal propellers use the excess power, that is not used by the vertical propellers to accelerate the aircraft. With higher speeds, the wing generates more lift and the power at the vertical propellers can be reduced. After approx. 11 seconds, the wing generates enough lift to turn off the vertical propellers. They are then locked in an aerodynamic optimal position for horizontal flight. With further acceleration, the angle of attack is reduced and then the profile of the morphing wing is slowly changed into cruise configuration to enable efficient cruise flight.

2.5. The Hybrid Configuration

Due to the VTOL capability, surges in the power demand occur, which only last for a short amount of time (less than one minute). Furthermore, INFERNO has more propellers than on a conventional airplane (eight motors for vertical take-off and two for horizontal flight). Both of these factors are ideal for installing a hybrid energy system.
Fig. 8 shows a schematic overview of the energy system being installed in the aircraft. The eight propellers for vertical flight are powered by 250 kW electric motors, and the two propellers for horizontal flight use a 600 kW electric motor each. In the middle of the wing, the 60 kW h battery pack is placed. Behind the payload module, the generator and the power electronics are installed. The generator is directly powered by the turbine engine. A conventional turbogenerator (General Electric (GE) H85-100) powered with kerosene or Sustainable Aviation Fuel (SAF) is used, to keep the required ground support equipment and technological risk at a minimum. Due to the redundant energy system from the relatively high capacity battery and the turbine engine, no Auxiliary Power Unit (APU) was installed.

2.5.1. Powerplant Selection

The best and most efficient choice of powering an aircraft of up to 300 km h^{-1} are turboprops or turboshaft engines. Turboshaft enginges allow high power-to-weight ratios without losing most of their power at high altitudes. While piston engines would also be a suitable selection for low speeds, they are not designed for high altitudes and the shaft rotational speeds are

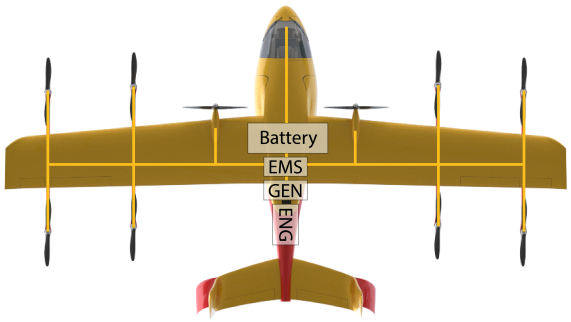

FIG 8. Illustration of the hybrid energy storage system

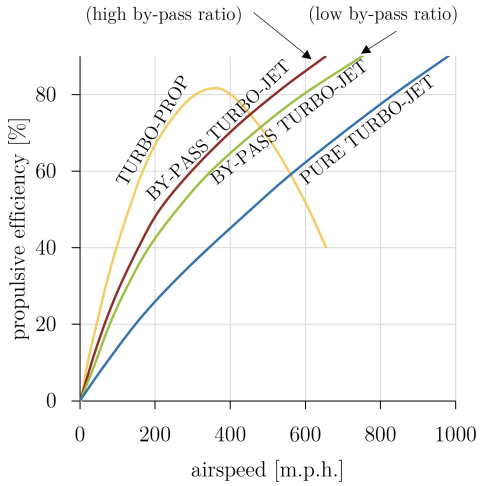

FIG 9. Propulsive efficiency comparison for various gas turbine engine configurations according to [26]

too low to adequately power a generator.
The INFERNO is powered by the GE H85-100 referenced as H85, as it is an optimal engine for all flight conditions. The H85 can use biofuels, also known as SAF [23]. Moreover, the H85 offers enhanced electronic engine control, which increases efficiency of the engine [24]. Additionally, turboprops allow excellent connection to power generators for a hybrid electric system, as described in chap. 2.5 and fig. 9, due to their high rotational speeds as present in other gas turbines. The SFC of the engine is estimated to be similar to other comparable engines like the GE-Catalyst, that offers a SFC of less than $300\,\mathrm{g\,kW^{-1}}$ [25].

Engine Data	H85-100
Overall length [mm]	1675
Overall width [mm]	590
Overall height[mm]	650
Dry mass [kg]	200
Maximum continuous power at sea level [kW]	634
Specific Fuel Consumption [kg/kWh]	<0.3

TAB 4. GE H85-100 Data [27]

2.5.2. Propeller and Electric Motor Selection

When selecting the propeller, it was decided to use products that are already available on the market. This brings advantages in terms of costs and availability. For the horizontal propulsion, the aircraft use two 5-bladed MTV-27 from MT-Propeller with a diameter of 82.7 in [28]. For the vertical lift, it features eight 2-bladed MTV-20 with a diameter of 200 cm [29]. Both types of propellers are constant speed propellers with variable pitch. The MTV-20 operates at 2700 rpm and the MTV-27 at 2200 rpm. The MTV-20 propellers are not specifically designed as lift propellers, because usually specific rotor blades are designed for the different types of helicopters and their missions as they strongly influence the drag in forward flight. The propeller profiles could, however, be exchanged or optimized at a later date if necessary.
No specific product was selected for the electric motors. There are already electric motors in the required power classes, but not yet optimized for aviation. However, with Wright Electric [15], a development is underway that is aiming to introduce electric motors for aviation from 500 kW to 4 MW power and a power-to-weight ratio of $10\,\mathrm{kW\,kg^{-1}}$ by 2026 [15]. A 2 MW motor is already in the testing phase. Since this company is working with major partners such as NASA, it is likely that the availability by 2030 is ensured. For the volume and mass calculation, reference product sheets from existing motors of the company YASA were used [30]. The estimated mass of the uninstalled generator is $7\,\mathrm{kW\,kg^{-1}}$ (including Power Electronics) ([31], [32]), with a 600 kW generator, this leads to a mass of 85 kg and the specific energy density of the electric motors was estimated with $12\,\mathrm{kW\,kg^{-1}}$[31].

2.5.3. Battery Sizing

At the start of the battery sizing process, several feasibility factors in the form of requirements for the battery concept were defined. These factors pertain mainly to the in-flight energy consumption demands of the electric motors during VTOL and SCOOP maneuver and are listed as following:

- Available installation space and mass budget constraints
- Battery capacity: 60 kW h
- High specific energy and energy density
- Very high charge-discharge rate (C-Rate)
- Market availability
- Operational life (cycles)

Initial power consumption calculations, during all different flight modes, with a 60 kW h battery pack concluded maximum required electrical power $P_{\mathrm{E_{max}}}$ at $1238.39\,\mathrm{kW}_e$. The integrated battery pack, as mentioned earlier, shall sustain $P_{\mathrm{E_{max}}}$ for an approximated 1 min duration of VTOL / SCOOP, for which, the required maximum C-Rate of 20C was calculated. An

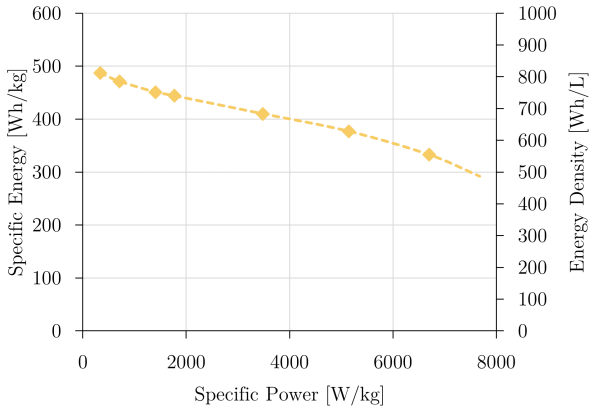

FIG 10. High power Licerion® cell energy across different C-Rates according to [33]

off-the-shelf battery pack with 20C discharge rate and a considerably high specific energy is still a few years ahead in the future. Therefore, as an initial practical approach to the sizing process, the calculations defining the battery dimensions were executed by developing a conceptual battery pack using the commercially available Sion Power Licerion® High Energy Density Cells. The design properties of individual Licerion® pouch cells are presented in tab. 5. The cell's parametric behaviour across multiple C-Rates is represented in fig. 10 adapted from [33], wherein at cell-level, the approximated values for specific energy and energy density at peak power consumption are 340 $\mathrm{W\,h\,kg^{-1}}$ and 560 $\mathrm{W\,h\,L^{-1}}$ respectively. These values are further used for determining the mass and volume of the cells that are to be integrated into the battery pack. The theoretical cumulative volume of the cells in the INFERNO battery pack was calculated to be approximately, 107 L and the approximated cumulative mass was calculated as 176 kg. The total battery pack mass also comprises a mass build-up factor that takes into consideration the mass of battery casing, battery management system, wires, and the battery pack's thermal management system [34]. Adapted from [34] and also confirmed in a brief conversation with a Sion Power battery engineer, a mass build-up factor of 1.4 was approximated for determining the energy and physical properties of the pack at battery-level. The total battery pack mass and volume were calculated to be 246 kg and, 150 L respectively. Tab. 5 gives a detailed overview of the relevant properties at cell-level and battery-level.

Ongoing research at Sion Power in 2018 estimated new Licerion® technology in 2022 to have significantly improved overall properties at cell level. The 2022 awaited Licerion® cells with a nominal specific energy and energy density of the 650 $\mathrm{W\,h\,kg^{-1}}$ and 1300 $\mathrm{W\,h\,L^{-1}}$ respectively, could lead to a (nominal) theoretical battery mass of as low as 129 kg and a theoretical volume of 65 L respectively, resulting in a better fuel economy, increased operation life and payload capability. At peak power consumption (20C) assuming 75% energy capacity delivery, the mass, and volume at battery-level are presumed to be at 185 kg and 92 L respectively [33]. The 2018 battery-level physical properties protrude over the mass budget restrictions and the 2022 battery-level values are significantly lower in comparison, but still slightly exceed the desired mass budget. A literature report on battery advancement trends made available by NASA shows that the specific energy of a cell at 270 $\mathrm{W\,h\,kg^{-1}}$ in 2018 could be projected at 690 $\mathrm{W\,h\,kg^{-1}}$ by 2030 with an annual increase rate of 8% at cell-level [35]. A similar trend, with an 8% annual increase rate, extrapolated for the 2018 Licerion® technology with current 340 $\mathrm{W\,h\,kg^{-1}}$ estimates the cell-level specific energy to be 856 $\mathrm{W\,h\,kg^{-1}}$ and 582 $\mathrm{W\,h\,kg^{-1}}$ at battery-level (32% loss from cell to pack) by 2030 with the battery pack weighing just about 103 kg. In order to keep the battery pack out of the critical component's list for the EIS and to account for additional fasteners and cables, the battery pack was estimated at 400 $\mathrm{W\,h\,kg^{-1}}$, which leads to a gross mass of 150 kg. At EIS, this relaxed requirement can lead to a cell with higher cycle life or more cells, which leads to a lower C-Rate and thus improves cycle life as well [36].

	Build-Up Factor = 1.4*			
	Cell-Level		Battery-Level	
Properties (at 20C)	2018	2022	2018	2022
Specific Energy [Wh/kg]	340	455*	244*	324*
Energy Density [Wh/L]	560	910*	400*	652*
Unit Mass [kg]	176	132*	246*	185*
Unit Volume [l]	107	66*	150*	92*

TAB 5. Sion Power Licerion battery properties at cell-level and pack-level for years 2018 and 2022 [33]; * represents mathematically / scientifically backed presumptions

2.5.4. Fuel Tank Sizing

The amount of fuel required for the design point was calculated as part of the performance calculation. In order to verify whether the space provided for fuel in the outer area of the wing span is sufficient, the tank volume V_{Kr} is estimated. For this purpose, a statistical procedure according to Torenbeek [37] is used for the preliminary design. This will have to be reviewed at a later stage of development. In order to take into account the installation space used by the battery, the calculation is carried out with the aid of a comparative wing (wing area S_{W}), which only represents the outer 6 m of the half-span b. It was assumed that no fuel can be accommodated in the winglets. λ describes the taper of the comparison wing and $\frac{t}{c}$ the thickness ratio at wing root. Using eq. (15), this results in a maximum

tank volume of 1391 L.

$$V_{\mathrm{Kr}} = 0,54 \cdot \frac{{S_{\mathrm{W}}}^2}{b} \cdot \left(\frac{t}{c}\right)_{\mathrm{i}} \cdot \frac{1+\lambda\sqrt{\tau}+\lambda^2\tau}{(1+\lambda)^2} \quad \text{with} \quad \tau = \frac{\left(\frac{t}{c}\right)_{\mathrm{a}}}{\left(\frac{t}{c}\right)_{\mathrm{i}}} \tag{15}$$

The calculated value was reduced by 30% to ensure the needed space for the morphing wing's actuators. The maximum available fuel volume is therefore 974 L, which corresponds to 780 kg of JET A-1 ([38]).

2.5.5. Engine Air Intake and Exhaust

The engine is supplied with air from both sides via air intakes see fig. 11. They are positioned high enough to prevent splash water from getting in. Unlike other aircraft, the exhaust gases are not discharged directly behind the engine out of the air frame, but are routed to the rear through the tail boom, where they flow out. The air flow is also shown in fig. 2. The exhaust gas flow is used to reduce the drag of the fuselage via wake filling, which is currently the subject of research. The CENTRELINE project [39] is investigating the possibility of increasing efficiency by introducing additional energy centrally at the tail. One of the findings is, that not too much thrust in relation to the total thrust is required to reduce fuselage drag significantly [40]. Even though INFERNO only uses the exhaust gas with its residual energy for Wake Filling, a noticeable drag reduction should be achieved. For detailed predictions, extensive CFD simulations are required. The exhaust pipe is made out of heat resistant materials, like nickel-chromium alloys [41]. Because the exhaust gas is discharged in the rear, the tailboom faces no hot exhaust temperature from the outside, like it would, if the exhaust gas is blown out closer to the engine. The CENTRELINE project is scheduled to have a EIS until 2035. However, INFERNO's wake filling is not of this magnitude and does not use an extra propulsion unit at the rear but only uses the remaining energy of the exhaust gas. Therefore technical maturity should be given until 2030.

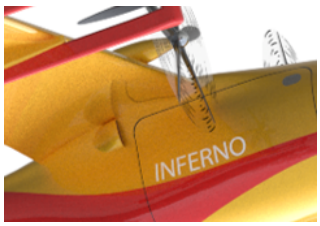

FIG 11. Engine Air inlets on both sides of the aircraft

2.6. Noise Reduction

There are several ways to reduce noise emissions of an aircraft. These options for noise reduction can be roughly divided into caused by the engine or the fuselage. However, it is not possible to influence the noise of the engine, as this is purchased directly from the manufacturer on the market, so no adjustments and optimizations are possible here. However, the engine is installed completely enclosed within the fuselage and therefore the noise can be shielded. The noise of the airframe, on the other hand, can be divided into 3 categories. These are the wing including the tail surfaces and the fuselage, the high-lift devices and the landing gear [42].
The targeted optimum is the clean configuration. Since the morphing wing completely eliminates high-lift devices, maximum noise reduction is achieved in this section. For the landing gear, there are concepts with optimized fairings to avoid hard edges in the air flow. However, as this leads to an increase in weight, and the landing gear is only used when landing at the airport, but not when taking up water in lakes, this measure was dispensed with.

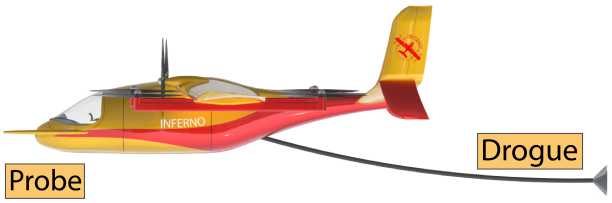

FIG 12. Drogue-and-probe concept for aerial refueling and maximizing firefighting time

2.6.1. Formation Flight

To increase the efficiency of the fleet on longer routes and to reduce emissions, formation flight is used. Savings of up to 18 % for the following aircraft have already been demonstrated in flight tests [43], [44]. However, flight controllers available today for automated formation flight are only stable outside the wake vortex inflow area [45]. For this reason, formation flight should be carried out within the center field. This corresponds to a distance of 15 to 150 wingspan of the aircraft. This area also has the advantage that the aircraft structure is significantly less stressed. However, the savings potential here is only up to 10 % [46], [47]. The exact sweep spot is to be found during the further development process with the help of a suitable simulation method. As a further development step, the loyal wingman concept is imaginable.

2.6.2. Aerial Refueling

INFERNO has a very large wing and can therefore store more fuel chap. 2.5.4, than required for the optimal 1200 km range. If, for example, the operational base for refueling is further away than in the design mission and there should be no payload limitations. The flight to and from the operational basis are very time-consuming and limit the dropped amount of water within a 24 h time slot. Due to its additional fuel tank capacity of 330 l an optional aerial refueling mechanism can be installed. With aerial refueling, only one out of the two aircraft have to return to the base and thus the time at the fire can be increased by 80% without

payload limitations. After the fuel that was obtained by refueling is consumed, the second aircraft return to the base to fuel up and change the pilot. Fig. 12 shows the additional equipment that is installed on the aircraft, that are equipped with the aerial refueling mechanism.

3. CONCLUSION

Fighting wildfires is one of the major challenges rapidly gaining significance with global warming on the rise. The INFERNO aerial firefighting concept developed as a result of the DLR Design Challenge 2022 presents a state-of-the-art aircraft designed to efficiently respond to wildfire scenarios around the globe. The concept features profound technologies to guarantee the best possible flight characteristics for these demanding missions. Thus, the INFERNO concept combines the flexibility of a VTOL aircraft with a conventional fixed-wing concept for efficiency during cruise. Water can be refilled during hovering (submerging part of the hull) and scooping during forward flight, leading to broad possibilities during various wildfire missions. The INFERNO aircraft is equipped with a serial hybrid system featuring a fuel efficient engine, a modern generator and a state-of-the-art battery concept supplying 10 electrically driven propeller, eight for the VTOL capabilities and two for the propulsion during forward flight. Moreover, the design is equipped with a modular fuselage part which can be flexible changed between the water tank, a passenger or a cargo module. Thus, an efficient year round fleet concept was developed minimizing ground times and operating costs. Additionally, a specific operational concept for 4 INFERNO aircraft during the INFERNO firefighting missions was designed optimizing the amount of water carried and dropped during the operation.

References

[1] P. Hirschberger, "WÄLDER IN FLAMMEN - Ursachen und Folgen der weltweiten Waldbrände," 2012.

[2] Umweltbundesamt, *Waldbrände*, 6.07.2022. [Online]. Available: https://www.umweltbundesamt.de/daten/land-forstwirtschaft/waldbraende#waldbrande-in-deutschland (visited on 07/06/2022).

[3] Deutsches Zentrum für Luft- und Raumfahrt, "DLR Design Challenge 2022," 2022. [Online]. Available: https://www.dlr.de/content/en/downloads/2022/dlr-design-challenge-2022-task-v1-4.pdf;jsessionid=1E9F991938632DEABC9C0D06235AD568.delivery-replication1?__blob=publicationFile&v=4 (visited on 07/06/2022).

[4] Johannes Ritter, Hannes Kahlo, Nicolas Mandry, Ahmet Günay Can, Prishit Modi, Benjamin Knoblauch, Johannes Schneider, Andreas Strohmayer, Tobias Dietl, Patrick Ratei, Prajwal Shiva Prakasha, Björn Nagel, "Design of a next generation vtol firefighting aircraft: Dlr design challenge 2022," 2022.

[5] D. Finger, "Vergleichende Leistungs- und Nutzenbewertung von VTOL- und CTOL-UAVs," *Luft- und Raumfahrt*, vol. 2017, pp. 44–47, Jan. 2017.

[6] A. Bacchini and E. Cestino, "Electric VTOL Configurations Comparison," *Aerospace*, vol. 6, no. 3, 2019, ISSN: 2226-4310. DOI: 10.3390/aerospace6030026. [Online]. Available: https://www.mdpi.com/2226-4310/6/3/26.

[7] L. Gaines, J. Sullivan, A. Burnham, and I. Belharouak, "Life-cycle analysis of production and recycling of lithium ion batteries," *Transportation Research Record*, vol. 2252, no. 1, pp. 57–65, 2011. DOI: 10.3141/2252-08. eprint: https://doi.org/10.3141/2252-08. [Online]. Available: https://doi.org/10.3141/2252-08.

[8] D. J. Roskam, *Airplane Design Part III: Layout of Cockpit, Fuselage, Wing and Empennage: Cutaways and Inboard Profiles*. Darcoperation, 2017, ISBN: 188488556X.

[9] D. Z. für Luft-und Raumfahrt, *100 Prozent nachhaltiger Kraftstoff zeigt Perspektive für Passagierflugzeuge*, 6.07.2022. [Online]. Available: www.dlr.de/content/de/artikel/news/2021/04/20211129_100-prozent-saf-kraftstoff-zeigt-perspektive-fuer-passagierflugzeuge.html (visited on 07/06/2022).

[10] M. Greenwood, J. M. Wrogemann, R. Schmuch, H. Jang, M. Winter, and J. Leker, "The battery component readiness level (bc-rl) framework: A technology-specific development framework," *Journal of Power Sources Advances*, vol. 14, p. 100 089, 2022, ISSN: 2666-2485. DOI: https://doi.org/10.1016/j.powera.2022.100089. [Online]. Available: https://www.sciencedirect.com/science/article/pii/S2666248522000075.

[11] Seitz, Arne and Habermann, Anaïs Luisa and Peter, Fabian and Troeltsch, Florian and Castillo Pardo, Alejandro and Della Corte, Biagio and van Sluis, Martijn and Goraj, Zdobyslaw and Kowalski, Mariusz and Zhao, Xin and Grönstedt, Tomas and Bijewitz, Julian and Wortmann, Guido, "Proof of concept study for fuselage boundary layer ingesting propulsion," *Aerospace*, vol. 8, no. 1, 2021, ISSN: 2226-4310. DOI: 10.3390/aerospace8010016. [Online]. Available: https://www.mdpi.com/2226-4310/8/1/16.

[12] M. Rendon, C. Sanchez, J. Gallo, and A. Anzai, "Aircraft hybrid-electric propulsion: Development trends, challenges and opportunities," *Sba Controle & Automacao Sociedade Brasileira de Automatica*, Jun. 2021. DOI: 10.1007/s40313-021-00740-x.

[13] D. Li, S. Zhao, A. Da Ronch, *et al.*, "A review of modelling and analysis of morphing wings," *Progress in Aerospace Sciences*, vol. 100, pp. 46–62, 2018, ISSN: 0376-0421. DOI: https://doi.org/10.1016/j.paerosci.2018.06.002. [Online]. Available: https://www.sciencedirect.com/science/article/pii/S0376042117301835.

[14] MTU AEROREPORT, *Modulare Flugzeuge: Flexibilität soll Kosten sparen*. [Online]. Available: https://aeroreport.de/de/innovation/modulare-flugzeuge-flexibilitaet-soll-kosten-sparen (visited on 07/06/2022).

[15] W. Electric, *Electric motor*. [Online]. Available: https://weflywright.com/technology#motors (visited on 07/05/2022).

[16] *LiDAR Scanners and Sensor Applications at RIEGL USA*. [Online]. Available: https://www.rieglusa.com/lidar-scanners-and-sensors-applications.html (visited on 07/11/2022).

[17] *Flightcell DZMx*, 2020. [Online]. Available: https://www.flightcell.com/products/flightcell-dzmx (visited on 07/11/2022).

[18] Prof. Dr.-Ing. Andreas Strohmayer, *Flugzeugentwurf I*.

[19] S. Gudmundsson, *General aviation aircraft design: Applied methods and procedures*, 1st ed. Oxford, UK: Butterworth-Heinemann, 2014, ISBN: 978-0-12-397308-5.

[20] B. G. van der Wall, *Grundlagen der Hubschrauber-Aerodynamik* (VDI-Buch), 1st ed. Berlin, Germany: Springer-Verlag, 2015, ISBN: 978-3-662-44400-9. DOI: https://doi.org/10.1007/978-3-662-44400-9.

[21] Xiaolong Zhang, Cheryl L. Bowman, Tim C. O'Connell, and Kiruba S. Haran, "Preliminary design of the superconducting rotor for nasa's high-efficiency megawatt motor," *IET Electric Power Applications*, 2017.

[22] J. J. Dr. Scheidler, "Large electric machines for aircraft electric propulsion," NASA, 2018.

[23] G. E. Aviation, *Future of flight*, G. Aviation, Ed. [Online]. Available: https://www.geaviation.com/future-of-flight (visited on 07/05/2022).

[24] G. E. Aviation, *H-Series Turboprop engine family — Engines on a mission*, G. Aviation, Ed. [Online]. Available: https://www.geaviation.com/propulsion/regional-business/h-series (visited on 07/05/2022).

[25] Peter deBock, *GE Turbines and small Engines Overview*, General Electric, Ed., 2019. [Online]. Available: https://arpa-e.energy.gov/sites/default/files/14_deBock_GETurbinesandsmallenginesoverview-ARPA-eINTEGRATEV2.pdf#page=8 (visited on 07/11/2022).

[26] P. Z. S. Spakovszky, "Implications of propulsive efficiency for engine design," D. Quattrochi, Ed., [Online]. Available: http://web.mit.edu/16.unified/www/FALL/thermodynamics/notes/node82.html (visited on 07/05/2022).

[27] European Union Aviation Safety Agency, *TYPE-CERTIFICATE DATA SHEET No.E.070 for M601/H80 series engines*, EASA, Ed. [Online]. Available: https://www.easa.europa.eu/downloads/7685/en (visited on 07/05/2022).

[28] European Union Aviation Safety Agency, *TYPE-CERTIFICATE DATA SHEET No. P.104 for MTV-27 series propellers*, EASA, Ed. [Online]. Available: https://www.mt-propeller.com/pdf/TCDS_EASA/MTV-27.pdf (visited on 07/05/2022).

[29] European Union Aviation Safety Agency, *TYPE-CERTIFICATE DATA SHEET No. EASA.P.100 for MTV-20 series propellers*, EASA, Ed. [Online]. Available: https://www.mt-propeller.com/pdf/TCDS_EASA/MTV-20.pdf (visited on 07/05/2022).

[30] YASA, *Yasa-750r electric motor product sheet*. [Online]. Available: https://www.yasa.com/wp-content/uploads/2021/05/YASA-750RDatasheet-Rev-11.pdf (visited on 07/06/2022).

[31] J. Benzaquen, J. He, and B. Mirafzal, "Toward more electric powertrains in aircraft: Technical challenges and advancements," *CES Transactions on Electrical Machines and Systems*, vol. 5, no. 3, pp. 177–193, 2021. DOI: 10.30941/CESTEMS.2021.00022.

[32] M. Hepperle, "Electric flight - potential and limitations," in *Energy Efficient Technologies and Concepts of Operation*, Oct. 2012. [Online]. Available: https://elib.dlr.de/78726/.

[33] Mikhaylik, Y., Kovalev, I., Scordilis-Kelley, Y., Liao, L., Laramie, M., Schoop, U., and Kelley, T., *650 Wh/Kg, 1400 Wh/L Rechargeable Batteries for New Era of Electrified Mobility*. [Online]. Available: https://www.scribd.com/document/467075308/650-whkg-1400-whl-recharg-batt-new-era-elect-mobility-ymikhaylik-0-pdf (visited on 07/02/2022).

[34] SUAVE: An Aerospace Vehicle Environment for Designing Future Aircraft, *Sizing*. [Online]. Available: https://suave.stanford.edu/doxygen/group__Methods-Power-Battery-Sizing.html (visited on 07/05/2022).

[35] A. Misra, "Summary of 2017 NASA Workshop on Assessment of Advanced Battery Technologies for Aerospace Applications," in *AIAA SciTech Forum and Exposition*, 2018.

[36] S. N. Motapon, E. Lachance, L.-A. Dessaint, and K. Al-Haddad, "A generic cycle life model for lithium-ion batteries based on fatigue theory and equivalent cycle counting," *IEEE Open Journal of the Industrial Electronics Society*, vol. 1, pp. 207–217, 2020. DOI: 10.1109/OJIES.2020.3015396.

[37] E. Torenbeek, *Advanced Aircraft Design: Conceptual Design, Analysis and Optimization of Subsonic Civil Airplanes*. John Wiley & Sons, 2013, ISBN: 978-1-118-56811-8.

[38] T. Energies, *Sicherheitsdatenblatt gemäß Verordnung (EG) Nr. 1907/2006 JET A-1*, 2018. [Online]. Available: https://services.totalenergies.de/sites/g/files/wompnd2336/f/atoms/files/sicherheitsdatenblatt_jet_a1.pdf.

[39] CENTRELINE, *Centreline website*. [Online]. Available: https://www.centreline.eu/innovation/ (visited on 07/10/2022).

[40] A. Seitz, F. Peter, J. Bijewitz, A. Habermann, Z. Goraj, M. Kowalski, A. Pardo, C. Hall, F. Meller, R. Merkler, O. Petit, S. Samuelsson, B Corte, M. Sluis, G. Wortmann, M. Dietz, "Concept validation study for fuselage wake-filling propulsion," Bauhaus Luftfahrt e.V., Warsaw University of Technology, University of Cambridge, Airbus Innovations, MTU Aero Enignes, Chalmers University of Technology, Technical University of Delft, Siemens AG, ARTTIC, 2018.

[41] S. Metals, *Inconel alloy 625*. [Online]. Available: https://www.specialmetals.com/documents/technical-bulletins/inconel/inconel-alloy-625.pdf (visited on 07/11/2022).

[42] G. M. L. David P. Lockard, "The airframe noise reduction challenge," 2004.

[43] M. Vachon, R. Ray, K. Walsh, and K. Ennix, "F/a-18 performance benefits measured during the autonomous formation flight project," Oct. 2003. DOI: 10.2514/6.2002-4491.

[44] C. Hanson, J. Ryan, M. Allen, and S. Jacobson, "An overview of flight test results for a formation flight autopilot," in *AIAA Guidance, Navigation and Control Conference and Exhibit*, [Reston, Va.]: [American Institute of Aeronautics and Astronautics], 2002, ISBN: 978-1-62410-108-3. DOI: 10.2514/6.2002-4755.

[45] A. K. R. Luckner, "Formationsflug von Verkehrsflugzeugen zur Treibstoffeinsparung," [Online]. Available: https://www.dglr.de/publikationen/2016/370376.pdf (visited on 07/01/2022).

[46] S. R. Bieniawski, S. Rosenzweig, and W. B. Blake, "Summary of flight testing and results for the formation flight for aerodynamic benefit program," in *52nd Aerospace Sciences Meeting*, ser. AIAA SciTech Forum, Reston, Virginia: American Institute of Aeronautics and Astronautics, 2014, ISBN: 978-1-62410-256-1. DOI: 10.2514/6.2014-1457.

[47] T. C. Flanzer and S. R. Bieniawski, "Operational analysis for the formation flight for aerodynamic benefit program," in *52nd Aerospace Sciences Meeting*, Reston, Virginia: American Institute of Aeronautics and Astronautics, 2014. DOI: 10.2514/6.2014-1460.

Contact address:

info@inferno-firefighting.info